Post-print version:

Automatic glucose control during meals and exercise in type 1 diabetes: Proof-of-concept in silico tests using a switched LPV approach

P. H. Colmegna, F. D. Bianchi, and R. S. Sánchez-Peña

This work has been published in **IEEE Control System Letters**:

P. H. Colmegna, F. D. Bianchi, and R. S. Sánchez-Peña, "Automatic glucose control during meals and exercise in type 1 diabetes: Proof-of-concept in silico tests using a switched LPV approach", *IEEE Control System Letters*, vol. 5, pp. 1489–1494, 2021.

Final version available at:

URL: https://ieeexplore.ieee.org/document/9273055

DOI: 10.1109/LCSYS.2020.3041211

BibTex:

```
@Article{Colmegna2021,
    Title    = {Automatic glucose control during meals and exercise in type 1
       diabetes:  Proof-of-concept in silico tests using a switched LPV approach},
    Author   = {Patricio H. Colmegna, Fernando D. Bianchi, and Ricardo S.
       Sánchez-Peña},
    Journal  = {IEEE Control System Letters},
    Year     = {2021},
    Number   = {5},
    Pages    = {1489--1494},
    Volume   = {5},
    Doi      = {10.1109/LCSYS.2020.3041211}
}
```

Automatic glucose control during meals and exercise in type 1 diabetes: Proof-of-concept in silico tests using a switched LPV approach

P. H. Colmegna, F. D. Bianchi, and R. S. Sánchez-Peña, *Senior Member, IEEE*

***Abstract*— Keeping the blood glucose levels within the safe range during meals and exercise still represents a major hurdle not only for patients with type 1 diabetes (T1D), but also for Artificial Pancreas (AP) systems. One of the reasons a fully (autonomous) closed-loop solution has not been released onto the market yet is the slow action of current insulin analogs. To partially overcome this limitation, the authors have previously designed a switched control strategy equipped with an insulin-on-board (IOB) safety loop that mitigates meal-related glucose excursions without carbohydrate counting. In this paper, a similar strategy based on a Linear Parameter-Varying (LPV) control law has been adapted to safely handle also exercise challenges with minimum user intervention. *In silico* results using the UVA/Padova simulator evidence that the proposed closed-loop scheme is feasible under moderate-intense exercise bouts by effectively and safely reducing the risk of hypoglycemia.**

***Index Terms*— Artificial pancreas, physical activity, switched LPV control, unannounced meals.**

I. Introduction

THE ultimate goal of an Artificial Pancreas (AP) system is to provide fully automated blood glucose control for patients with Type 1 Diabetes (T1D). Generally, a minimally invasive approach is used, where both glucose measurement and insulin infusion are performed subcutaneously via a Continuous Glucose Monitoring (CGM) sensor and a Continuous Subcutaneous Insulin Infusion (CSII) pump.

The design of an AP controller encounters several problems such as delays and errors, both in glucose measurement and insulin infusion, model nonlinearities, and large inter– and intrapatient uncertainties. Nowadays, the main limitation for AP systems is the significant delay introduced by current insulin analogs that can lead to insulin stacking, limiting the achievable performance of glucose controllers. The reader is referred to [1] and [2] for a complete review of these challenges.

Although numerous AP studies were performed around the world (a recent worldwide update can be found in [3]), there are only two commercial insulin pumps with AP systems, and both still require patient intervention during meals and exercise: the Minimed 670G [4], and the Tandem t:slim x2 with Basal-IQ/Control-IQ [4]–[6].

Moderate-intensity exercise is particularly challenging to control, because it triggers an increase in subject's insulin sensitivity that can last several hours. Due to the slow dynamics of current insulin analogs, guidelines recommend patients on pumps reduce their basal rates up to two hours prior to exercise and consume carbohydrates to prevent exercise-induced hypoglycemia [7]. However, this approach should be taken cautiously to avoid carbohydrate over-consumption and lack of insulin that can ultimately lead to hyperglycemia. Previous AP strategies that address this problem can be found in [8]–[13] and a recent survey, in [14].

The strategy adopted in this work is mainly based on previous work by the authors, but with the addition of a series of innovations that aim at reducing patient burden by minimizing their intervention in the closed-loop strategy. To this end, an inner Switched Linear Parameter Varying (SLPV) controller that has two operating modes: one conservative and one aggressive [15], [16], is combined with an outer sliding-mode safety layer (SAFE) that limits the controller's action based on the residual active insulin (or IOB) [17]. This is the first time that the SLPV is combined with the SAFE layer, since in previous *in silico* and *in vivo* studies, the inner controller was represented by a switched Linear Quadratic Gaussian (LQG) controller [18], [19].

There is an undeniable compromise between patient's autonomy and closed-loop performance, particularly subject to disturbances. The announced/unannounced disturbances play an important role in patient's autonomy. The contribution of this work is a proof-of-concept group of simulations performed using the Food and Drug Administration (FDA)-accepted UVA/Padova metabolic simulator under multiple meal and exercise disturbances. It tests and validates the feasibility of the proposed AP system without meal announcement and/or Carbohydrate (CHO) count, considering the performance degradation when exercise is not announced.

In this work, Hyperglycemia Detection (HD) module commands which control mode is selected. When persistent hyperglycemia is detected, for instance, after a meal ingestion, the controller switches into the aggressive mode and the IOB constraint is relaxed, allowing the AP system to inject more

This work was supported by Nuria (Argentina) and Cellex (Spain) Foundations, and JDRF (2-APF-2019-737-A -N). The second author has a starting Research Grant from ITBA. Funding sources had no active involvement in the development of this work.

P. H. Colmegna is with Center for Diabetes Technology, University of Virginia and CONICET (e-mail: pc2jx@virginia.edu).

F. D. Bianchi and R. S. Sánchez-Peña are with the Instituto Tecnológico de Buenos Aires (ITBA) and CONICET (e-mails: febianchi@itba.edu.ar, rsanchez@itba.edu.ar).

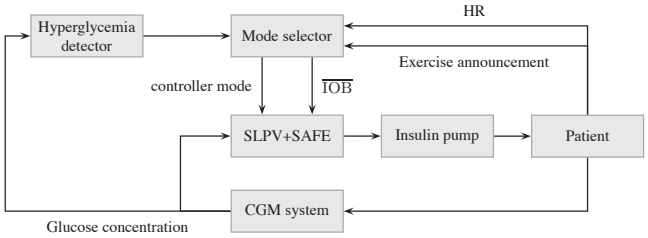

Fig. 1. Block diagram of the AP strategy. HR: Heart Rate, $\overline{\text{IOB}}$: Insulin On Board constraint, SAFE: Safety Auxiliary Feedback Element, SLPV: Switched LPV.

insulin and quickly mitigate the glucose excursion. Also, a new Mode Selection (MS) algorithm has been added to combine the HD module with Heart Rate (HR) data[1], and automatically adjust the controller's settings in case of meals and/or exercise.

The paper is organized as follows: Section II briefly describes previous work in which this procedure is based, and presents the new modules that have been added to the AP strategy. Sections III and IV present the simulations and the resulting conclusions, respectively.

II. Control Strategy Design

A sketch of the new proposed AP strategy is presented in Fig. 1. At the core of the scheme are the SLPV controller and SAFE layer. Every five minutes, this controller computes an insulin dose and the SAFE limits, if a predefined IOB limit is going to be violated, the control signal to minimize the risk of hypoglycemia. The novelty in this new approach is the MS algorithm that modifies the SLPV and SAFE settings according to meal and exercise data.

A. Switched LPV controller

The SLPV strategy consists of two controllers $K_j(\rho)$ with $j \in \{1,2\}$ that are designed for the control-oriented LPV model presented in [20]:

$$G(\rho): \begin{cases} \dot{x}(t) = A(\rho)x(t) + Bu(t-\tau) \\ g(t) = Cx(t) \end{cases} \tag{1}$$

where the input u corresponds to the subcutaneous insulin infusion (in pmol/min) and the output g is the glucose concentration deviation (in mg/dl) obtained from the CGM, and

$$A(\rho) = \begin{bmatrix} 0 & 1 & 0 \\ 0 & 0 & 1 \\ 0 & -p_2p_3 & -(p_2+p_3) \end{bmatrix} + \rho \begin{bmatrix} 0 & 0 & 0 \\ 0 & 0 & 0 \\ -p_2p_3 & -(p_2+p_3) & -1 \end{bmatrix},$$

$$B = \begin{bmatrix} 0 & 0 & 1 \end{bmatrix}^T, \quad C = k \begin{bmatrix} z & 1 & 0 \end{bmatrix}.$$

Parameters z, p_2, p_3, and τ are fixed to population values ($z = 0.1501$, $p_2 = 0.0138$, $p_3 = 0.0143$, and $\tau = 15$), k is a constant based on the patient's Total Daily Insulin (TDI)

[1]An alternative without the use of an HR monitor could also be explored as indicated in [13], but will not be developed here.

TABLE I
Parameter values of $\rho(g)$ of (2).

i	q_i	r_i	s_i	t_i
1	0	0	-3.432×10^{-6}	4.470×10^{-3}
2	0	9.058×10^{-8}	-5.356×10^{-5}	1.135×10^{-2}
3	-4.238×10^{-8}	1.140×10^{-5}	-9.167×10^{-4}	2.584×10^{-2}
4	0	1.732×10^{-4}	-2.308×10^{-2}	7.712×10^{-1}
5	0	0	-2.833×10^{-5}	1.408×10^{-2}

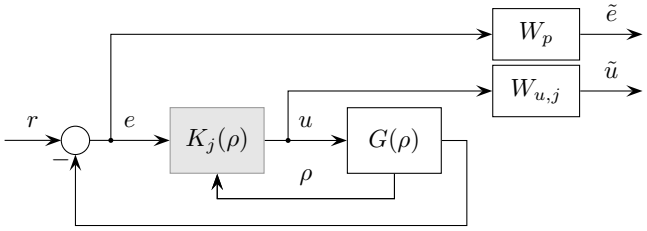

Fig. 2. LPV control design setup for each $K_j(\rho)$ with $j \in \{1,2\}$.

[20], and ρ is a piecewise-polynomial function of the measured glucose concentration:

$$\rho(g) = q_i g^3 + r_i g^2 + s_i g + t_i, \tag{2}$$

where:

$$i = \begin{cases} 1 & \text{if } 300 \text{ mg/dl} \leq g \\ 2 & \text{if } 110 \text{ mg/dl} \leq g < 300 \text{ mg/dl} \\ 3 & \text{if } 65 \text{ mg/dl} \leq g < 110 \text{ mg/dl} \\ 4 & \text{if } 59 \text{ mg/dl} \leq g < 65 \text{ mg/dl} \\ 5 & \text{if } g < 59 \text{ mg/dl}. \end{cases} \tag{3}$$

and the polynomial coefficients are given in Table I. Parameter τ represents an average delay in insulin appearance in the subcutaneous depot from where insulin is slowly absorbed into plasma (see [21], [22]).

Controller $K_1(\rho)$ performs slight changes on the basal insulin infusion rate, whereas $K_2(\rho)$ responds more aggressively to glucose changes and is triggered only when hyperglycemia is detected. The LPV control design setup is shown in Fig. 2, where $\tilde{e}$ and $\tilde{u}$ are obtained after weighting the glucose error $e = r - g$ and the control action u (insulin infusion) with the following weights:

$$W_p(s) = 100\,\frac{10s+1}{5000s+1}, \tag{4}$$

$$W_{u,j} = k_{u,j}, \tag{5}$$

Index $j \in \{1,2\}$ corresponds to the controller mode in the switching strategy ($k_{u,1} = 0.07$ and $k_{u,2} = 0.5$). Weight $W_p(s)$ penalizes glucose deviations from the basal value r (around 120 mg/dl), and weight W_u penalizes changes in insulin delivery [16]. Note that the LPV model $G(\rho)$ is affine in the parameter ρ, therefore each controller $K_j(\rho)$ can be computed with tools like `hinfgs` available in Matlab. The controller switching is implemented as indicated in [23].

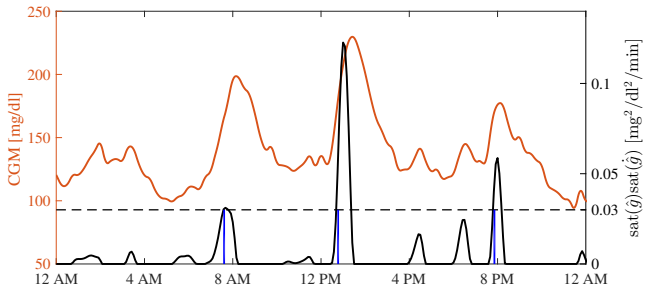

Fig. 3. Example of how the HD module works. The blue bars indicate when hyperglycemia is detected and the controller switches into the aggressive mode. The dash black line indicate the threshold of 0.03 mg^2/dl^2/min.

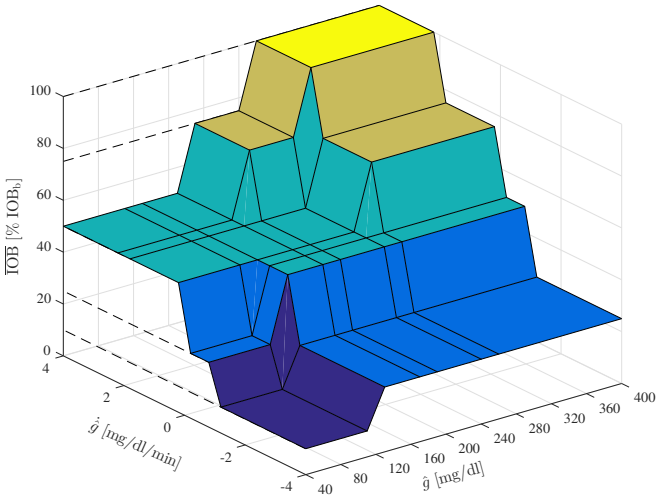

Fig. 4. $\overline{\text{IOB}}$ surface as a function of g and $\dot{g}$. The $\overline{\text{IOB}}$ is expressed as percentage of IOB_b.

B. SAFE unit

The SAFE unit is a sliding-mode safety layer that adapts the SLPV controller's gain based on IOB constraints. Its aim is to maintain the estimated IOB below a predefined patient-specific constraint, indicated as $\overline{\text{IOB}}$. For this purpose, this unit produces a signal $\gamma \in [0,\ 1]$ that modulates the insulin imposed by the SLPV controller. A detailed description of this safety layer can be found in [17] and [18]. As in [18], it is considered that $\overline{\text{IOB}}_\text{s} = \text{IOB}_\text{b}$ + 40 g/CR and $\overline{\text{IOB}}_\text{m} = \text{IOB}_\text{b}$ + 55 g/CR, where $\overline{\text{IOB}}_\text{b}$ is the estimated IOB value at basal input rate and CR is the subject-specific insulin-to-carbohydrate ratio in U/g. In this work, the constraint $\overline{\text{IOB}}$ is set by the MS unit as will be described in the next section.

C. Hyperglycemia detection module

The HD module determines which LPV controller should be selected based on the following algorithm. Current glucose value and rate of change are estimated using the Kalman filter presented in [24]. Estimated glucose concentration $\hat{g}$ and its derivative $\dot{\hat{g}}$ are saturated at zero (only positive values are considered), and multiplied together $\text{sat}(\hat{g}) \cdot \text{sat}(\dot{\hat{g}})$ in order to reflect the joint magnitude increase of both variables. The output is a signal that will be approximately zero most of the time, except when glucose rapidly increases where a peak will be observed. If the size of the peak surpasses 0.03 mg^2/dl^2/min, the HD module will indicate that the aggressive mode should be selected. It is important to highlight that the goal of this module is not to perfectly detect meal events, but to detect hyperglycemic situations that require a more aggressive response of the controller. For safety purposes, the HD is blocked during the night or when the exercise mode is active. An example of how the HD works is presented in Fig. 3.

D. Heart rate model

In this work, the first-order exercise model in [25] is used to relate treadmill velocity v to HR:

$$\text{HR} = \frac{k_\text{HR}}{\tau_\text{HR} s + 1} v \tag{6}$$

This model represents deviations around linearized values for both v and HR, in the absence of low frequency (upward) drift of HR, as observed during prolonged moderate-vigorous intensity running. Since results show that there are small differences in the identified parameters for moderate and intense levels, the mean value of k_HR and τ_HR parameters will be considered in the upcoming simulations, i.e. $k_\text{HR} = 24.2$ bpm/(m/s), $\tau_\text{HR} = 57.6$ sec. Given those parameters, velocity v is estimated to reach a HR of 120 bpm (2 times the basal HR) in accordance with what is reported in [26].

E. Mode selection module

The MS unit supervises the controller to prevent hyper- and hypoglycemia events after meals and exercise. This unit gathers HR data, an exercise announcement signal provided manually by the patient, and information from the HD module. After processing these data, two outputs are generated: the switching signal j for the SLPV controller, and the Insulin on Board (IOB) limit ($\overline{\text{IOB}}$) for the SAFE layer. The mode selection is implemented as a logic unit with several timers. This unit takes into account HR measurements, exercise announcement and meal detection, and keeps records of the time in each mode in order to decide which mode must be applied. Stability is evaluated by using the same methodology as in a previous result by the authors [23], i.e., computing a Single Quadratic Lyapunov Function (SQLF) for each controller in order to guarantee closed loop stability under arbitrary switching amongst controllers [27].

Four operation modes are included:

1) *Conservative mode:* The conservative controller $K_1(\rho)$ is used in combination with $\overline{\text{IOB}} = \overline{\text{IOB}}_\text{s}$.
2) *Aggressive mode:* When hyperglycemia is detected, the LPV controller is switched to $K_2(\rho)$, and $\overline{\text{IOB}}$ is set to $\overline{\text{IOB}}_\text{m}$.
3) *Exercise mode:* The exercise mode is triggered when the patient announces exercise at $t_\text{ex} - t_\text{an}$, with t_ex the exercise start time and t_an the anticipation time. This mode remains active for 60 minutes if no exercise is detected or until 60 min after the end of the detected

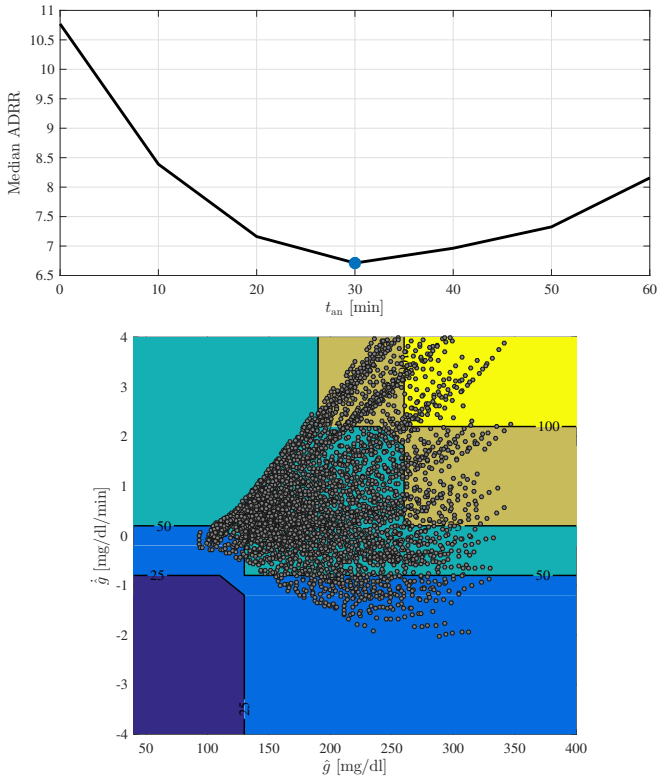

Fig. 5. **Top:** Median ADRR values for different anticipation times. The blue dot highlights the optimal t_{an}. **Bottom:** $\overline{IOB}$ surface projection onto the $\hat{g}$ and $\dot{\hat{g}}$ axes. Each dot represents the estimated glucose condition at $t_{ex} - t_{an}$.

exercise bout. During this mode the LPV controller is switched to K_1 and $\overline{IOB}$ is set to a fixed value obtained from the surface illustrated in Fig. 4. As shown, $\overline{IOB}$ during the exercise mode will be a percentage of IOB_b, depending on the estimated glucose concentration $\hat{g}$ and its derivative $\dot{\hat{g}}$ at the moment exercise is announced.

4) *Post-exercise mode:* To minimize the risk of hypoglycemia as a consequence of an increased in insulin sensitivity, the exercise mode is followed by a post-exercise mode in which $\overline{IOB}$ is set to $\overline{IOB}_s$ for the following 8 hours. Nonetheless, switching to the aggressive controller is still allowed during this mode to reduce risk of hyperglycemia when detected.

F. Optimal anticipation time estimation

In order to determine the optimal t_{an} that minimizes both risks of hypo- and hyperglycemia, 8-hour experiments were carried out considering the 10 *in silico* subjects of the distribution version of the UVA/Padova simulator integrated with the exercise model reported in [26]. Each *in silico* subject underwent a 30-minute long moderate exercise bout under multiple initial conditions for different t_{an} times, ranging from 0 to 60 min in 10 min steps. Current glucose value and rate of change were estimated from the Kalman filter, and $\overline{IOB}$ was set using the surface presented in Fig. 4. Results are illustrated in Fig. 5. The bottom plot indicates where glucose conditions laid in the $\hat{g}$-$\dot{\hat{g}}$ plane when exercise was announced. For each

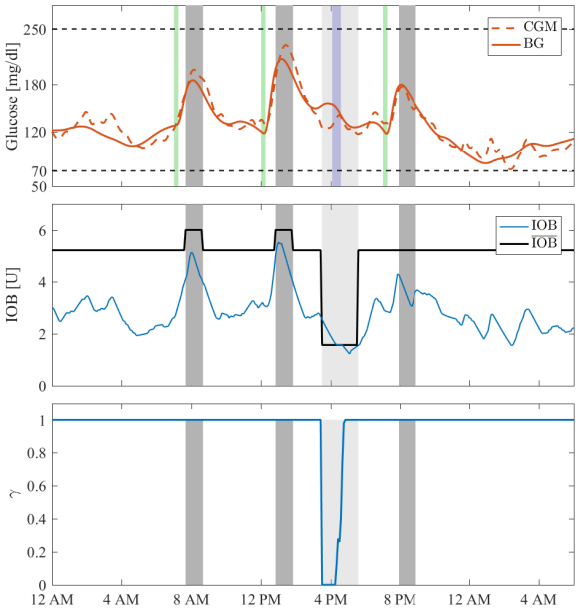

Fig. 6. Closed-loop response for Adult #1. Green bars represent the meal times, dark grey regions indicate when the aggressive mode is selected, light grey regions, when the exercise mode is active and blue regions, the exercise period.

experiment, the Average Daily Risk Range (ADRR) value [28] was computed to obtain an index that weights both hypo- and hyperglycemia risks. In the top plot of Fig. 5, the median ADRR values are plotted against the evaluated t_{an} values. Note that the minimum ADRR is obtained with $t_{an} = 30$ min; if $t_{an} < 30$ min, the risk of hypoglycemia increases, while if $t_{an} > 30$ min, the risk of hyperglycemia increases.

III. Results

Simulations have been carried out for all 10 *in silico* adults of the distribution version of the UVA/Padova simulator with three meals:

- 40 g meal at 7 AM,
- 70 g meal at 12 PM, and
- 60 g meal at 7 PM

a 30-min bout of moderate exercise at 4 PM, which is announced to the controller with an anticipation of 30 minutes, and no hypo-treatments. Although no intraday variability is included in this version of the simulator, the authors have previously considered it from the control standpoint: as uncertainty in [16] and as a time-varying parameter in an LPV control-oriented model in [29]. Therefore, the current implementation can be extended in a straightforward manner to handle intraday variations. Also, it is worth highlighting that simulations include measurement noise, and that robustness is accounted for by inter-patient variability, both implemented already in the UVa/Padova simulator.

In order to show how the control system works, an individual closed-loop response is illustrated in Fig. 6. There, meals are represented by the green bars, and exercise is indicated by the blue region. The dark gray regions indicate when

TABLE II

AVERAGE CLOSED-LOOP RESULTS FOR ALL *in silico* ADULTS WITH THE PROPOSED CONTROL STRATEGY FOR BASELINE AND CASES 1 TO 3. LGBI: LOW BLOOD GLUCOSE INDEX, HBGI: HIGH BLOOD GLUCOSE INDEX, IQR: INTERQUANTILE RANGE. [28].

	Baseline			Case 1			Case 2			Case 3		
Overall	**Mean**	**Median**	**IQR**	**Mean**	**Median**	**IQR**	**Mean**	**Median**	**IQR**	**Mean**	**Median**	**IQR**
Average blood glucose (mg/dl)	131.5	131.5	5.4	133.2	133.5	5.1	125.6	125.3	4.4	128.3	127.9	5.0
Coefficient of variation (%)	24	25	5	25	25	4	26	26	5	25	25	5
% time $<$ 70 mg/dl	0	0	0	0	0	0	1.4	0	2	0	0	0
% time in $[70, 140]$ mg/dl	68.2	68.6	6.8	65.9	65.7	9.7	71.2	71.2	8.2	71.3	72.2	6.3
% time in $[70, 180]$ mg/dl	89.0	90.3	9.6	88.0	89.6	6.1	90.4	90.4	5.6	90.9	92.8	7.4
% time $>$ 180 mg/dl	11.0	9.7	9.6	12.0	10.4	6.1	8.2	5.7	5.4	9.1	7.3	7.4
LBGI	0.23	0.20	0.20	0.32	0.32	0.31	0.62	0.59	0.59	0.45	0.35	0.32
HBGI	2.30	2.08	0.68	2.49	2.38	0.68	1.92	1.73	0.68	2.06	1.77	0.44
Exercise period (3 PM - 7 PM)												
Average blood glucose (mg/dl)	128.1	127.5	10.9	141.0	139.6	17.6	112.7	112.8	10.6	132.4	130.5	15.6
Coefficient of variation (%)	15	16	6	7	7	7	28	26	6	11	12	5
% time $<$ 70 mg/dl	0	0	0	0	0	0	8.1	0	9.5	0	0	0
% time in $[70, 140]$ mg/dl	69.4	69.3	27.0	52.7	62.9	62.7	64.9	66.4	22.0	71.6	69.9	22.0
% time in $[70, 180]$ mg/dl	98.1	100	0	98.1	100	0	90.0	94.4	16.6	98.1	100	0
% time $>$ 180 mg/dl	1.9	0	0	1.9	0	0	1.9	0	0	1.9	0	0
LBGI	0.09	0.08	0.14	0	0	0	2.24	2.03	0.93	0.01	0	0.01
HBGI	1.40	1.21	0.97	2.13	1.79	2.04	1.21	1.11	0.94	1.47	1.15	1.12

the aggressive controller K_2 is selected, and the light gray regions, when the exercise mode is active. It is clear how the $\overline{\text{IOB}}$ modulation is instrumental in keeping the glucose level within safe margins. After meals, $\overline{\text{IOB}}$ is increased to allow the aggressive controller to inject more insulin if needed. Instead, in the region where exercise is announced, the IOB limit is lowered to make the controller reduce the insulin infusion in advance, preventing exercise-related hypoglycemia. Note that $\overline{\text{IOB}}$ implies only a limit and not the exact amount of insulin to be commanded by the AP system[2].

Complete results have been structured in four cases:

- Baseline: no exercise – unannounced
- Case 1: no exercise – announced
- Case 2: exercise – unannounced
- Case 3: exercise – announced

Closed-loop responses for all these cases are illustrated in Fig. 7. As expected, exercise-induced hypoglycemia is observable in Case 2, whereas in all other cases, glucose values remain within safe bounds.

Average closed-loop results for all *in silico* adults are grouped in Table II-F based on time consensus outcome metrics for glucose controllers' performances described in [31]. In Case 2, greater time in hypoglycemia is observed, specially in the time interval between 3 PM and 7 PM, reaching a mean percentage of time below 70 mg/dl of 8.1%. This increase in the risk of hypoglycemia is also accompanied by a marked increase in the coefficient of variation (CV), mainly caused by the delayed reaction of the controller to exercise-induced hypoglycemia. It is worth highlighting that even when exercise is announced but not performed (Case 1), the mean increase in time spent in hyperglycemia (% time $>$ 180 mg/dl) with respect to baseline is negligible (overall: 1%, 3 PM - 7 PM: 0%). This desired behavior is, in part, due to the fact that the Exercise mode is terminated after 60 min if no exercise

[2]An ongoing research collaboration of the authors is the exploration of a time-varying adaptive IOB limit, like the one presented in [30].

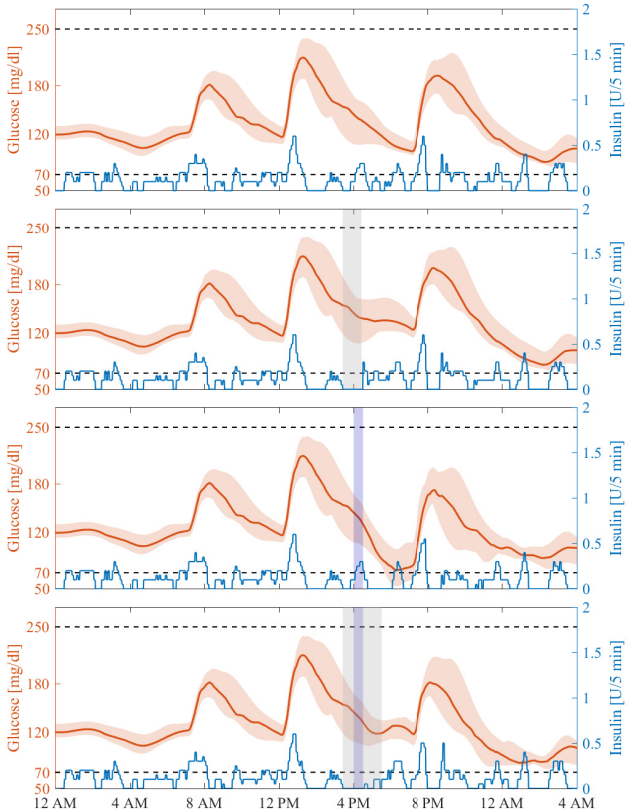

Fig. 7. Closed-loop responses for baseline (upper) and cases 1 to 3 (lower) with the proposed closed-loop strategy. The thick lines are the median values (glucose and insulin), and the boundaries of the filled areas are the 5th and 95th percentiles (glucose). The gray region reflects the time in exercise mode and the blue area, the exercise period. The dashed black lines indicate the boundaries of the target zone [70-180] mg/dl.

is detected. Here, Case 2 quantifies the compromise between patient's autonomy (not involved in announcing exercise), *vs* performance (increase in the risk of hypoglycemia).

IV. Conclusions

In this paper, a previous AP strategy was adapted for safely controlling glucose under exercise challenges. When the patient announces that he/she will exercise, the SAFE layer automatically adjusts the IOB limit, $\overline{\text{IOB}}$, based on the current glucose value and rate of change. This allows the controller to take precautionary action and compensate for delays in insulin action. *In silico* results using the FDA-accepted UVA/Padova simulator were obtained, showing the efficacy of the proposed strategy under multiple meal and exercise conditions. In addition, the performance degradation when exercise is not announced is also accounted for to illustrate that given the slow dynamics of current insulin analogs, there is still an undeniable compromise between patient's autonomy and closed-loop performance that has to be taken into account as a starting point in any AP design.

References

[1] G. M. Steil, A. E. Panteleon, and K. Rebrin, "Closed-loop insulin delivery-the path to physiological glucose control," *Adv. Drug Deliv. Rev.*, vol. 56, no. 2, pp. 125–144, Feb 2004.

[2] B. W. Bequette, "Challenges and recent progress in the development of a closed-loop artificial pancreas," *Annu. Rev. Control*, vol. 36, no. 2, pp. 255–266, Dec 2012.

[3] R. Sánchez-Peña and D. Cherñavvsky, Eds., *The Artificial Pancreas: Current Situation and Future Directions*. Academic Press, 2019.

[4] "Minimed 670G system - P160017/S031," https://www.fda.gov/medical-devices/recently-approved-devices/minimed-670g-system-p160017s031, accessed: 2020-08-28.

[5] "t:slim X2 insulin pump with Basal-IQ technology - P180008," https://www.fda.gov/medical-devices/recently-approved-devices/tslim-x2-insulin-pump-basal-iq-technology-p180008, accessed: 2020-08-28.

[6] "FDA authorizes first interoperable, automated insulin dosing controller designed to allow more choices for patients looking to customize their individual diabetes management device system," https://www.fda.gov/news-events/press-announcements/fda-authorizes-first-interoperable-automated-insulin-dosing-controller-designed-allow-more-choices, accessed: 2020-08-28.

[7] M. C. Riddell, I. W. Gallen, C. E. Smart, C. E. Taplin, *et al.*, "Exercise management in type 1 diabetes: a consensus statement," *Lancet Diabetes Endocrinol*, vol. 5, no. 5, pp. 377–390, 2017.

[8] M. D. Breton, D. R. Cherñavvsky, G. P. Forlenza, M. D. DeBoer, *et al.*, "Closed-loop control during intense prolonged outdoor exercise in adolescents with type 1 diabetes: The artificial pancreas ski study," *Diabetes Care*, vol. 40, no. 12, pp. 1644–1650, 2017.

[9] L. M. Huyett, T. T. Ly, G. P. Forlenza, *et al.*, "Outpatient closed-loop control with unannounced moderate exercise in adolescents using zone model predictive control," *Diabetes Technol Ther*, vol. 19, no. 6, pp. 331–339, 2017.

[10] J. E. Pinsker, A. J. L. Sanz, J. B. Lee, M. M. Church, *et al.*, "Evaluation of an artificial pancreas with enhanced model predictive control and a glucose prediction trust index with unannounced exercise," *Diabetes Technol Ther*, vol. 20, no. 7, pp. 455–464, 2018.

[11] K. Turksoy, I. Hajizadeh, N. Hobbs, J. Kilkus, *et al.*, "Multivariable artificial pancreas for various exercise types and intensities," *Diabetes Technol Ther*, vol. 20, no. 10, pp. 662–671, 2018.

[12] C. M. Ramkissoon, A. Bertachi, A. Beneyto, J. Bondia, and J. Vehi, "Detection and control of unannounced exercise in the artificial pancreas without additional physiological signals," *IEEE J Biomed Health Inform*, vol. 24, no. 1, pp. 259–267, 2020.

[13] J. Garcia-Tirado, P. Colmegna, J. P. Corbett, B. Ozaslan, and M. D. Breton, "In silico analysis of an exercise-safe artificial pancreas with multistage model predictive control and insulin safety system," *J Diabetes Sci Technol*, vol. 13, no. 6, pp. 1054–1064, 2019.

[14] S. Tagougui, N. Taleb, J. Molvau, É. Nguyen, M. Raffray, and R. Rabasa-Lhoret, "Artificial pancreas systems and physical activity in patients with type 1 diabetes: challenges, adopted approaches, and future perspectives," *J Diabetes Sci Technol*, vol. 13, no. 6, pp. 1077–1090, 2019.

[15] P. Colmegna, R. Sánchez-Peña, R. Gondhalekar, E. Dassau, and F. Doyle III, "Reducing glucose variability due to meals and postprandial exercise in T1DM using switched LPV control: In silico studies," *J. Diabetes Sci. Technol.*, vol. 10, no. 3, pp. 744–753, March 2016.

[16] F. D. Bianchi, M. Moscoso-Vásquez, P. Colmegna, and R. S. Sánchez-Peña, "Invalidation and low-order model set for artificial pancreas robust control design," *J Process Contr*, vol. 76, pp. 133 – 140, 2019.

[17] A. Revert, F. Garelli, J. Picó, H. De Battista, P. Rossetti, J. Vehi, and J. Bondía, "Safety auxiliary feedback element for the artificial pancreas in type 1 diabetes," *IEEE Trans. Biomed. Eng.*, vol. 60, no. 8, pp. 2113–2122, Aug. 2013.

[18] P. Colmegna, F. Garelli, H. De Battista, and R. Sánchez-Peña, "Automatic regulatory control in type 1 diabetes without carbohydrate counting," *Control Eng Pract*, vol. 74, pp. 22–32, 2018.

[19] R. Sánchez-Peña, P. Colmegna, F. Garelli, H. De Battista, *et al.*, "Artificial pancreas: Clinical study in Latin America without premeal insulin boluses," *J Diabetes Sci Technol*, vol. 12, no. 5, pp. 914–925, 2018.

[20] P. Colmegna, R. Sánchez-Peña, and R. Gondhalekar, "Linear parameter-varying model to design control laws for an artificial pancreas," *Biomed. Signal Process. Control*, vol. 40, pp. 204–213, Feb 2018.

[21] M. Schiavon, C. Dalla Man, and C. Cobelli, "Modeling subcutaneous absorption of fast-acting insulin in type 1 diabetes," *IEEE Trans Biomed Eng*, vol. 65, no. 9, pp. 2079–2086, 2017.

[22] G. Goodwin, M. M. Seron, A. M. Medioli, T. Smith, B. R. King, and C. E. Smart, "A systematic stochastic design strategy achieving an optimal tradeoff between peak bgl and probability of hypoglycaemic events for individuals having type 1 diabetes mellitus," *Biomed. Signal Process. Control*, vol. 57, 2020.

[23] P. Colmegna, R. S. Sánchez-Peña, R. Gondhalekar, E. Dassau, and F. J. Doyle III, "Switched LPV glucose control in type 1 diabetes," *IEEE Trans. Biomed. Eng.*, vol. 63, no. 6, pp. 1192–1200, June 2016.

[24] E. Dassau, B. Bequette, B. Buckingham, and F. J. Doyle III, "Detection of a meal using continuous glucose monitoring," *Diabetes Care*, vol. 31, no. 2, pp. 295–300, Feb 2008.

[25] J. Hunt, S. Fankhauser, and J. Saengsuwan, "Identification of heart rate dynamics during moderate-to-vigorous treadmill exercise," *Biomedical Engineering Online*, vol. 14:117, 2015.

[26] C. Dalla-Man, M. D. Breton, and C. Cobelli, "Physical activity into the meal glucose-insulin model of type 1 diabetes: In silico studies," *J Diabetes Sci Technol*, vol. 3, no. 1, pp. 56–67, 2009.

[27] D. Liberzon, *Switching in Systems and Control*. Boston: Birkhäuser, 2003.

[28] A. N. Pitsillides, S. M. Anderson, and B. Kovatchev, "Hypoglycemia risk and glucose variability indices derived from routine self-monitoring of blood glucose are related to laboratory measures of insulin sensitivity and epinephrine counterregulation," *Diabetes Technol Ther*, vol. 13, no. 1, pp. 11–17, 2008.

[29] F. D. Bianchi, M. Moscoso-Vásquez, P. Colmegna, and R. S. Sánchez-Peña, "Control-oriented model with intra-patient variations for an artificial pancreas," *IEEE J Biomed Health Inform*, vol. 24, pp. 2168–2194, 2020.

[30] E. Fushimi, C. Serafini, H. De Battista, and F. Garelli, "Automatic glycemic regulation for the pediatric population based on switched control and time-varying iob constraints: An in silico study," *Med Biol Eng Comput*, vol. 58, pp. 2325–2337, 2020.

[31] T. Danne, R. Nimri, T. Battelino, R. M. Bergenstal, *et al.*, "International consensus on use of continuous glucose monitoring," *Diabetes Care*, vol. 40, no. 12, pp. 1631–1640, 2017.